ELSEVIER

15 June 1997

Optics Communications 139 (1997) 107–116

OPTICS COMMUNICATIONS

Full length article

Laser controlled atom waveguide as a source of ultracold atoms

M.V. Subbotin, V.I. Balykin, D.V. Laryushin, V.S. Letokhov *

Institute of Spectroscopy, Russian Academy of Sciences, 142092 Troitsk, Moscow Region, Russia

Received 20 August 1996; revised 25 November 1996; accepted 8 January 1997

Abstract

This paper considers the channeling of atoms over a hollow tapering waveguide with an evanescent laser light wave formed on its inner surface, the frequency detuning of the wave being positive with respect to the atomic absorption line. Using inelastic reflection of the atoms from the evanescent light wave and tapering waveguide geometry makes it possible to reduce the temperature and increase the phase-space density of the ensemble of atoms being continuously injected into the waveguide from a magneto-optical trap by a factor of 10^5. It is suggested that the waveguide under consideration should be used to study the specific features of the quantum propagation of atoms over the waveguide and collective phenomena in quantum-mechanical systems of high density (the Bose–Einstein condensate), and also as a bright coherent source of cold atoms.

PACS: 32.80.Pj

1. Introduction

An atom placed in a quasiresonant laser field is acted upon by a dipole light pressure force which pulls the atom in, or pushes it out of the region of high field intensity, depending on the sense of the atomic polarizability at the optical frequency. The use of the gradient light pressure force is at the root of mirrors for atomic de Broglie waves, as well as other optical elements of atomic optics and interferometry, such as atomic lenses and various types of atomic traps, resonators, and waveguides (see reviews in Refs. [1–3]). Two schemes have been suggested and implemented to date for the channeling of atoms over an optical waveguide. The authors of Ref. [4] suggested using the fundamental optical mode of a hollow cylindrical waveguide containing laser light with a negative frequency detuning for the channeling of atoms drawn toward the waveguide axis by the gradient force. This proposal was successfully realized in Ref. [5]. It was proposed in Ref. [6] that use should be made of an evanescent light wave inside a hollow cylindrical optical fiber to make a waveguide for atoms. Atoms propagate in such a waveguide while reflecting from the evanescent light wave having a positive frequency detuning [7].

The elastic reflection of atoms from an evanescent light wave has been well studied, both theoretically [8,9] and experimentally [10–12]. In the case of reflection of atoms whose energy level system agrees well with the Λ-diagram (alkali metals), they managed to observe experimentally [13] the inelastic reflection of atoms predicted in Ref. [14], associated with their spontaneous transitions between hyperfine structure sublevels in the course of interaction with the evanescent wave. As demonstrated in Ref. [13], an atom may lose, in a single reflection event, up to 50% of its transverse kinetic energy with a probability of a few tens percent. It was suggested using the effect of inelastic reflection of atoms to cool and localize atoms in a gravitation trap [15]. The first attempt to observe reflection cooling in a hollow fiber was undertaken by the group at the University of Colorado [16]. In this work, we present a full treatment of the atomic phase-space density increase in a hollow tapering fiber, which was shortly described in Ref. [17], and propose to employ this effect to make a bright coherent source of ultracold atoms.

* Corresponding author. E-mail: lls@isan.msk.su.

PII S0030-4018(97)00102-8

The paper is organized as follows:

In Section 2.1 we consider the channeling and cooling of atoms in a plane waveguide and present the analytic relationship between the transverse part of the kinetic energy of an atomic ensemble and the longitudinal coordinate. In addition, we describe a computer model and find the lowest temperature attainable through this process. The question of optimal parameters of the evanescent wave laser is discussed, too. In Section 2.2 we consider the characteristic features of atomic propagation through a cylindrical waveguide. Using as an example a 2D tapering fiber (Section 2.3), we show the possibility of phase-space density increase in such a fiber and examine the problem of its optimal geometry from this point of view. These results are used in Section 2.4 to reveal the dependence of the phase-space density of an atomic ensemble in a 3D tapering hollow fiber and output thermodynamic parameters of the atomic gas on its longitudinal coordinate. In Section 3 we discuss some possible applications of the proposed cooling scheme: (a) investigation of the behavior of an ensemble of weekly interacting bosons near the point of condensation; (b) development of a bright coherent source of the de Broglie wave with a characteristic wavelength of the order of several tenths of microns (Section 3.2).

2. Increasing the phase-space density of an atomic ensemble in a hollow waveguide

2.1. Plane waveguide

It is convenient to begin by considering the evolution of an atomic ensemble in the one-dimensional case, where the simple analytical description is possible. Consider the behavior of an atom in a plane hollow waveguide formed by two parallel dielectric plates (Fig. 1) on whose inner

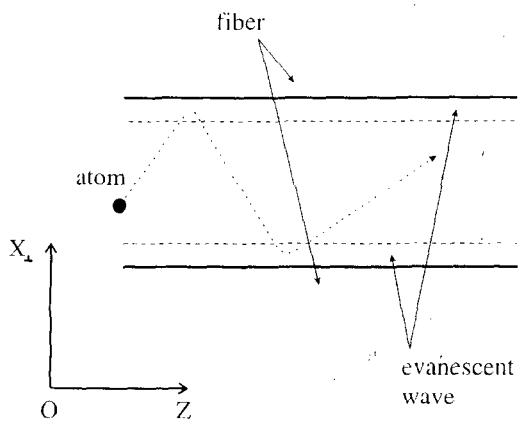

Fig. 1. Plane atomic waveguide. The atom channels over the waveguide while experiencing elastic and inelastic reflections from the evanescent light wave.

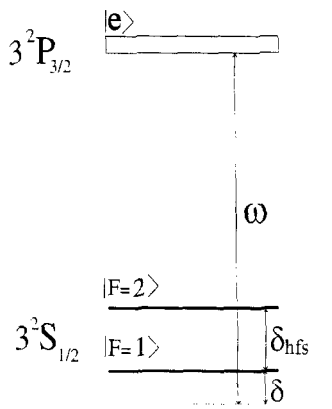

Fig. 2. Energy level diagram of the sodium atom and transitions ensuring the cooling of the atom upon reflection.

surfaces evanescent waves are formed with a positive frequency detuning for the transition between the lower hyperfine structure sublevel $|F=1\rangle$ and the excited state $|P\rangle$ of the sodium atom (Fig. 2). Assume that the waveguide is filled with light whose frequency is tuned to resonate with the transition $|F=2\rangle \leftrightarrow |P\rangle$ ("repumping" light). The evanescent waves provide for the reflection of the atom in the course of being channeled over the waveguide. This reflection may be either elastic (the atom remains in the state $|F=1\rangle$) or inelastic (the atom moves to the state $|F=2\rangle$). An atom in the state $|F=2\rangle$ residing outside the evanescent waves is moved back to the sublevel $|F=1\rangle$ by the repumping light.

Let the initial atomic velocity projection onto the waveguide axis be positive, and the transverse atomic velocity be other than zero. In that case, the atom will start to be channeled over the waveguide, while undergoing reflections from the evanescent waves. The average reduction of the transverse energy of the atom in a single reflection event is [15]

$$\langle \Delta E_\perp \rangle = \int_{-\infty}^{\infty} (U_1(r) - U_2(r))\, \Gamma_{12}\, dt = -\frac{2}{3}\,\frac{\delta_{HFS}}{\delta + \delta_{HFS}}\,\frac{M L \Gamma}{\hbar \delta}\,(1-q)\, v_\perp E_\perp , \qquad (1)$$

where U_1 and U_2 are the space-dependent light-induced shifts of the sublevels $|F=1\rangle$ and $|F=2\rangle$ in the evanescent wave, respectively, Γ_{12} is the rate of the transition from $|F=1\rangle$ to $|F=2\rangle$, L is the characteristic depth of penetration of the evanescent wave into the vacuum, q is the factor allowing for the atomic degeneracy in the angular momentum projection, Γ is the natural linewidth, δ is the detuning of the laser frequency from the frequency of the transition $|F=1\rangle \leftrightarrow |P\rangle$, δ_{HFS} is the hyperfine splitting, M is the mass of the atom, and $v_\perp$ is its transverse velocity. The average rate at which the atomic energy decreases in the waveguide is governed by its change in a

single reflection event and the time between two consecutive reflection events, $\Delta t = d/v_\perp$. Dividing both sides of Eq. (1) by Δt, we get the following expression for the average atomic energy reduction rate:

$$\frac{\langle \Delta E_\perp \rangle}{\Delta t} = -\frac{2}{3}\frac{\delta_{\mathrm{HFS}}}{\delta_{\mathrm{HFS}}+\delta}\frac{A}{d}\frac{\Gamma}{\delta}\frac{2E_\perp^2}{\hbar}. \tag{2}$$

Replacing in the above expression the ratio between the finite differences by the appropriate derivative, we obtain a differential equation for the rate of extraction from the transverse kinetic energy component $E_\perp$ of the atom in the course of its being channeled over the waveguide:

$$\dot{E}_\perp = -\frac{2}{3}\frac{\delta_{\mathrm{HFS}}}{\delta_{\mathrm{HFS}}+\delta}\frac{A}{a}\frac{\Gamma}{\delta}\frac{2E_\perp^2}{\hbar} \equiv -CE_\perp^2. \tag{3}$$

Having solved this equation subject to the initial condition $E_\perp(0) = E_{\perp 0}$, we get the relationship between the energy $E_\perp$ and the channeling time of the atom in the waveguide:

$$E_\perp(t) = \frac{1}{Ct + 1/E_{\perp 0}}. \tag{4}$$

Considering that the longitudinal atomic velocity $v_z = \mathrm{const}$ and $z = v_z t$, we may recast Eq. (4) in the form

$$E_\perp(z) = \frac{1}{Cz/v_z + 1/E_{\perp 0}}. \tag{5}$$

Eq. (5) holds true when the transverse kinetic energy of the atom is much higher than its recoil energy. Failure to allow for the recoil momentum leads to a wrong relationship $E_\perp(z)$ at large z values:

$$E_\perp(z) \underset{z=\infty}{\to} 0.$$

To reveal the behavior of the function $E_\perp(z)$ at small transverse kinetic energy values, we numerically integrated the equations of motion of the atom in the waveguide:

$$M\ddot{\boldsymbol{r}} = -\nabla U_{1,2,3}(\boldsymbol{r}) + \boldsymbol{f}(t), \tag{6}$$

where $U_{1,2,3}(\boldsymbol{r})$ is the potential energy of the atom in one of the "dressed" states [18] $|1\rangle$, $|2\rangle$, or $|3\rangle$ corresponding to the levels $|F=1\rangle$, $|F=2\rangle$, or $|P\rangle$:

$$U_1(\boldsymbol{r}) = \frac{\hbar}{2}\left(\sqrt{\delta^2 + \tfrac{2}{3}\Omega_{\mathrm{R}}^2(\boldsymbol{r})} - \delta\right), \tag{7a}$$

$$U_2(\boldsymbol{r}) = \frac{\hbar}{2}\left(\sqrt{(\delta+\delta_{\mathrm{HFS}})^2 + \tfrac{2}{3}\Omega_{\mathrm{R}}^2(\boldsymbol{r})} - \delta\right), \tag{7b}$$

$$U_3(\boldsymbol{r}) = -\frac{\hbar}{2}\left(\sqrt{\delta^2 + \tfrac{2}{3}\Omega_{\mathrm{R}}^2(\boldsymbol{r})} - \delta\right). \tag{7c}$$

$\boldsymbol{f}(t)$ is the term allowing for the change in the momentum of the atom upon a change in its quantum state, and Ω_{R} in Eqs. (7a)–(7c) is the Rabi frequency. When the atoms are channeled over a waveguide formed by an evanescent light wave with a positive frequency detuning, some of them may be lost as a result of, first, spontaneous decays and secondly subbarrier channeling. Both of these loss mechanisms were taken into account in our model by excluding from further consideration those atoms which reached the surface of the dielectric in the course of reflection. The validity of such an approach will be discussed below.

To allow for momentum diffusion and other effects associated with changes in the quantum state of the atom during its motion, use was made of the Monte Carlo random process modeling technique. At each numerical integration step, we computed the probability of the transition $|F=1\rangle \to |F=2\rangle$ and then compared it with a random quantity of the same density of distribution on the interval [0,1] and changed the quantum state of the atom or not, as was appropriate. The presence of the "repumping" laser radiation was taken into consideration as follows. All the atoms residing in the state $|F=2\rangle$ at a distance exceeding a few Λ from the dielectric surface were moved to the state $|F=1\rangle$. The change in the state of the atom was attended by the recoil momentum p_{rec} of four photons on average being imparted to it [15],

$$\boldsymbol{p}_{\mathrm{rec}} = \sum_{i=1}^{4}\hbar\boldsymbol{k}_i = \hbar\frac{2\pi}{\lambda}\sum_{i=1}^{4}\boldsymbol{\xi}_i, \tag{8}$$

where λ is the wavelength of the spontaneously emitted photon and $\boldsymbol{\xi}$ is a random unit vector.

To allow for tunneling, we computed for each event of reflection from the evanescent wave the probability p_{tun} that the atom will tunnel through the potential barrier produced by the wave [19]:

$$p_{\mathrm{tun}} = \frac{1}{1+e^{2D}}, \quad D = \frac{1}{2\pi}\frac{A}{\lambda}\frac{\left(v_{\perp\max}^2 - v_\perp^2\right)^{3/2}}{v_{\mathrm{recoil}}v_{\perp\max}^2}, \tag{9}$$

where v_{recoil} is the recoil velocity of the atom and $v_{\perp\max}$ is the maximum classical atomic velocity at which it still can reflect from the evanescent wave. As demonstrated in Ref. [6], the correction to p_{tun} introduced by the interaction between the polarized atom and the dielectric surface is small, the parameters in hand being what they are, so that the lifetime of the atom in the waveguide is reduced by a mere 10%. But this decrease can be compensated by increasing the laser intensity. We therefore disregarded this effect. An atom was assumed to have either settled on the waveguide wall and left the ensemble or reflected successfully, depending on the relationship between p_{tun} and a random quantity of the same density of distribution on the interval [0,1]. Both of the main mechanisms responsible for the loss of atoms were thus taken into account in our model.

As was experimentally observed in Ref. [20], the reflection cooling of sodium atoms in an evanescent wave has the highest efficiency if the laser detuning is approximately equal to the Rabi frequency $\Omega_{\mathrm{R}}(r_{\mathrm{turning}})$ at the turning point of the atomic trajectory. In the case of an incident sodium atom with an average velocity of 50 cm/s

the maximum rate of reflection cooling is achieved at a detuning of $\delta = 100$ MHz. The frequency $\Omega_R(r_{surface})$ is chosen to be 500 MHz, i.e. the height of the light potential barrier is greater than the average kinetic energy of the incident atom by a factor of 20. All the numerical results presented in the paper were obtained using this laser light parameters.

The modeling results are presented in Fig. 3. The squares show the computed mean absolute transverse atomic velocity values. The solid line is the result of a parametric adjustment by means of functions of the form

$$v_\perp(z) = v_{\perp\min} + \frac{B}{1 + Az}, \tag{10}$$

with the parameters $v_{\perp\min}$, A, and B. The parameter $v_{\perp\min}$ has the meaning of the ultimate transverse velocity whereto the mean transverse velocity of the atomic ensemble tends in a plane waveguide. The quantity $v_{\perp\min}$ determined the minimum temperature to which an atomic ensemble can be cooled in such a system. Expression (5) describes quite well the change of energy of an atom down to a value comparable with its recoil energy, but $E_\perp(t) \underset{t=\infty}{\to} E_{\perp\min} \neq 0$. In the case under consideration, $E_{\perp\min}$ is of the same order of magnitude as the kinetic atomic energy corresponding to three recoil momenta ($v_{\perp\min} \cong 10$ cm/s).

2.2. Cylindrical fiber

Let us now analyze by means of the above-described method the evolution of an atomic ensemble in a horizontal hollow cylindrical waveguide with an inside diameter of $d = 10$ μm and a length of $L = 0.8$ cm, which is shown schematically in Fig. 4, along with a typical trajectory of an atom therein. The initial conditions for the atomic

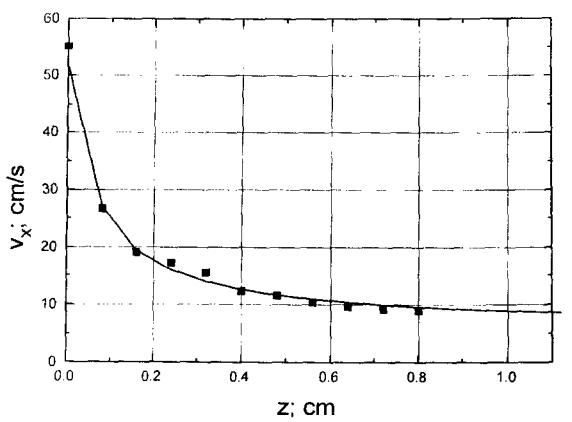

Fig. 3. Average transverse velocity component of atoms propagating over a plane waveguide as a function of the longitudinal coordinate. The squares indicate computer modeling results, and the solid line is the result of a parametric adjustment by means of fractional rational functions $v_\perp \underset{z\to+\infty}{\to} 7$ cm/s.

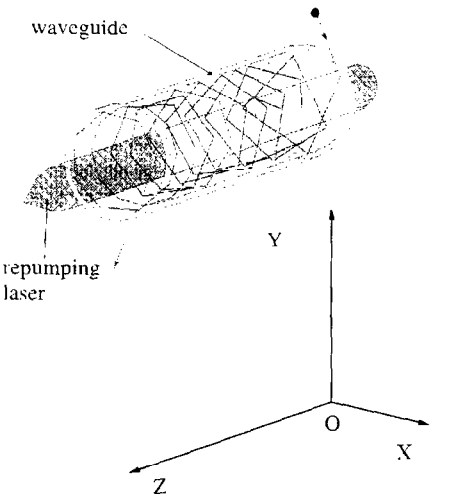

Fig. 4. Hollow cylindrical waveguide and a typical trajectory of an atom therein. Because the atom gradually loses its transverse kinetic energy component in the course of channeling over the waveguide, its trajectory clings closer and closer to the evanescent wave.

velocities and coordinates were selected as follows. The atoms were placed in the plane XOY at the beginning of the waveguide (see Fig. 4) so that their distribution over the cross-section of the waveguide was uniform: the longitudinal velocity v_z was equal to 50 cm/s for all atoms, and their distribution over the radial and azimuthal velocity components corresponded to a thermal distribution with a mean velocity of 50 cm/s. The atoms channel over the waveguide while experiencing numerous reflections from the evanescent wave. Some of them (around 30%) are of inelastic character and lead to a reduction of the radial atomic velocity component, its azimuthal counterpart remaining unchanged. As can be seen from Fig. 4, this causes the atomic trajectory to cling closer and closer to the evanescent wave, so that the atom eventually starts "rolling" over the wave. Note that this effect stops the atomic cooling process. It is apparently exactly this fact that prevented the authors of Ref. [16] from actually observing cooling of atoms in a cylinder waveguide. For this reason, the radial distribution of the atoms at the exit of the waveguide features a sharp peak near the surface of the dielectric (Fig. 5). One can also see from Fig. 5 that the radial atomic distribution at the exit of the cylindrical waveguide has narrowed perceptibly (approximately by a factor of 5).

Figs. 6a, 6b present the initial and final atomic distributions over the absolute radial and azimuthal velocity components in the cylindrical waveguide. A substantial (fivefold) cooling of the radial atomic velocity component as a result of inelastic reflections from the evanescent wave is evident from Fig. 6a. With the waveguide being 0.8 cm long, an atom undergoes some 30 reflections from the

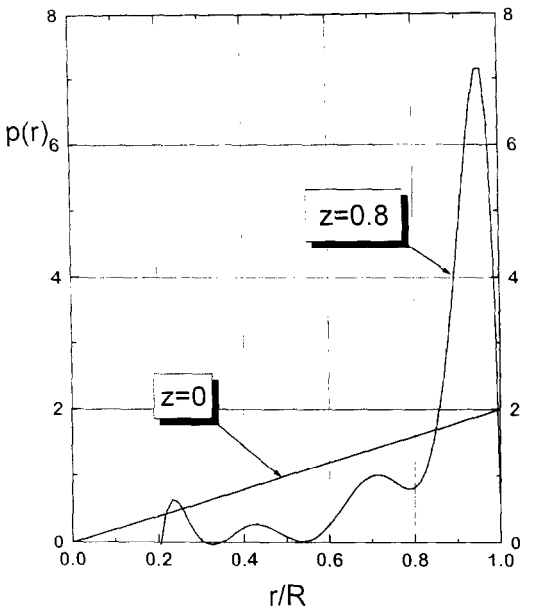

Fig. 5. Spatial distributions of atoms over the radius of a cylindrical waveguide at the entrance ($z = 0$) and exit ($z = 0.8$ cm). The initial atomic distribution, uniform over the entrance cross section of the waveguide, transforms into a distribution with a pronounced peak near the waveguide wall. The width of the exit distribution is approximately one-fifth of the entrance distribution.

evanescent wave. In that case, as follows from the curve of Fig. 3, a thermal equilibrium is established between the evanescent wave and the transverse atomic degree of freedom at a temperature of $T \cong 8 \times 10^{-6}$ K. The insignificant narrowing of the azimuthal velocity distribution (Fig. 6b) is explained by the coupling between the radial and azimuthal degrees of freedom due to the gravity force that disturbs the cylindrical symmetry. The extent of this coupling is determined by the parameter $\alpha = Mgd/E_{\perp \min}$ which in our case is equal to about 10^{-2}.

Fig. 7 shows the mean absolute radial atomic velocity as a function of the longitudinal coordinate z in the same way as Fig. 3 does for the case of a plane waveguide. In the case of cylindrical waveguide symmetry, the cooling limit of the transverse atomic velocity component is 7 cm/s. As can be seen, the characteristic waveguide length at which this limit is reached amounts to about 0.5 cm, which is somewhat less than in the case of a plane waveguide. The substantial narrowing of the radial spatial and velocity distributions in the cylindrical waveguide points to a principal possibility of using such schemes to increase the phase-space density of an atomic ensemble.

2.3. 2D hornfiber

The narrowing of the velocity and spatial distributions of atoms in an ensemble in the course of their channeling over a cylindrical waveguide points to the possibility of

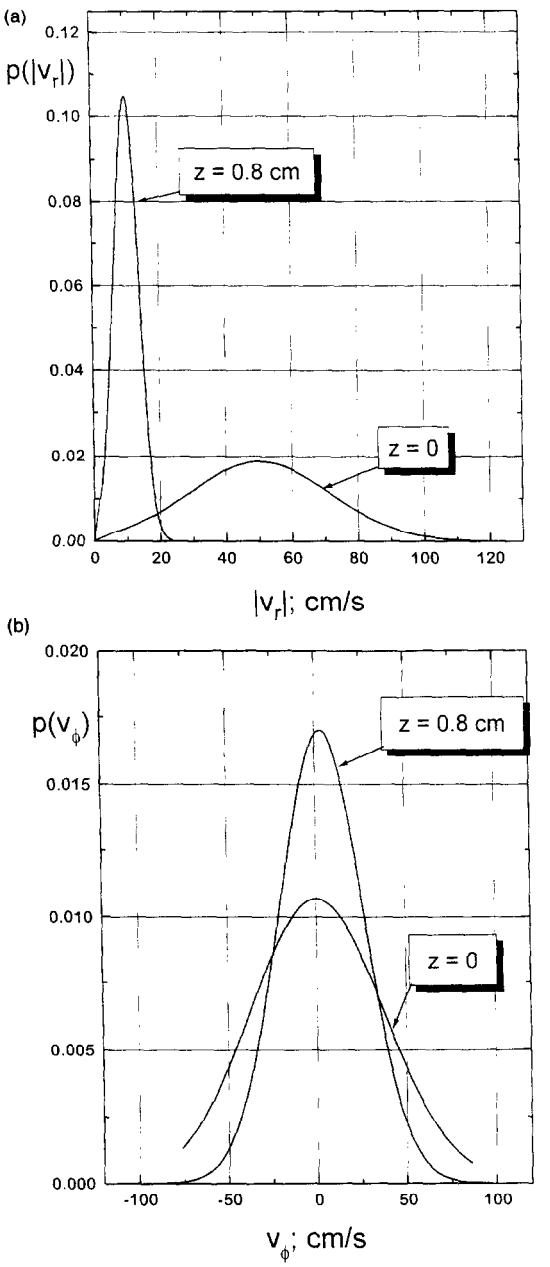

Fig. 6. (a) Absolute radial and (b) azimuthal velocity distributions of atoms at the entrance and exit of a cylindrical waveguide. The initial transverse and azimuthal atomic velocity distributions are of Maxwell type with a temperature of $k_B T = \hbar\Gamma$ (Doppler cooling limit) and the initial longitudinal atomic velocity distribution is of δ-type. (a) The exit atomic distribution has its average velocity corresponding to two recoil momenta approximately, which is around one-fifth the initial atomic velocity. (b) The azimuthal distribution has slightly narrowed because of the gravity force disturbing the axial symmetry and coupling together the radial and azimuthal degrees of freedom.

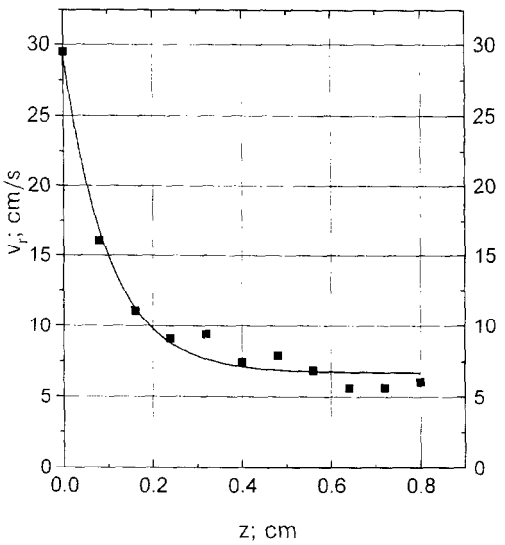

Fig. 7. Average transverse velocity component of atoms propagating over a cylindrical waveguide as a function of the coordinate z. The squares indicate computer modeling results, and the solid line is the result of a parametric adjustment by means of fractional rational functions $v_{\perp} \underset{z \to +\infty}{\to} 7$ cm/s.

using this effect to increase the atomic phase-space density. Consider for simplicity a two-dimensional curved tapering waveguide formed by two dielectric surfaces whose cross-sections at planes parallel to the plane YOZ are hyperbolas:

$$x(z) = \frac{A_{1,2}}{k_{1,2}z + 1} + B_{1,2}z + C_{1,2}, \qquad (11)$$

where $A_{1,2}$, $B_{1,2}$, $C_{1,2}$ and $k_{1,2}$ are parameters. Each of the hyperbolas has an asymptote forming some angle with the OZ-axis. The hyperbolas form a tapering two-dimensional hollow waveguide which at great z values can be well approximated by a cone with an apex angle of α (the taper angle of the waveguide) inclined at an angle of β with respect to the horizontal. The treatment of the two-dimensional problem takes a substantially less computer time and gives an understanding of the physical phenomena occurring in the 3D system at various parameters. Fig. 8 shows the 2D hornfiber and various types of atomic trajectories in it. We analyzed a waveguide with an entrance aperture diameter of 500 μm and an exit aperture diameter of 10 μm. Atoms at the initial instant of time were placed near the origin of the coordinates in the waveguide cavity and were imparted some initial velocity directed inside the waveguide. The absolute value of the velocity obeyed a thermal distribution with a mean value of 50 cm/s. The atoms channeled over the waveguide while undergoing numerous reflections from the evanescent wave. Because of the tapering of the waveguide and the effect of the gravity force, the atomic velocity projection onto the local waveguide axis varied in the course of channeling. The contributions from these two factors in the given waveguide geometry are opposite to each other. If there had been no dissipation in the system, an atom in the waveguide would have been observed to execute undamped oscillations with some frequency and a mean amplitude corresponding to its initial kinetic energy by the virial theorem.

The presence of a mechanism by which an atom in the waveguide loses some of its kinetic energy in inelastic reflections from the evanescent light wave causes the equilibrium position of the atom to move gradually downward. Depending on the relationship between the dissipation rate and the natural oscillation frequency of the atom, the system exhibits one of the following two modes of behavior typical for linear oscillatory systems: (i) oscillations damping over many periods of oscillation (see Fig. 8) and (ii) an exponential decay of the initial energy without oscillations. Fig. 8 also presents the trajectory of an atom

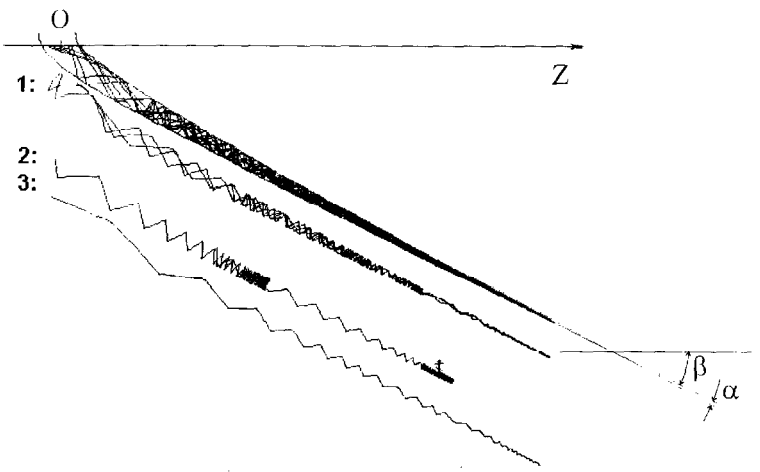

Fig. 8. Trajectories of atoms in a 2D hornfiber. 1 – damped oscillations; 2 – death through tunneling; 3 – strongly damped oscillations.

which has tunneled through the potential barrier formed by the evanescent light wave and "settled" on the waveguide wall. This fact is marked by a tombstone. One can also see from this figure that the density of the atomic trajectories increases as the waveguide narrows down, which means that the atomic phase-space density becomes higher. The oscillation free mode of channeling was found to be optimal to achieve the coldest possible output atomic ensemble at the fixed evanescent wave parameters and fiber length. This mode was realized by variation of the apex and the inclination angles (α and β respectively). We have estimated that the mean velocity of the atomic ensemble along the axis of the fiber was constantly decreasing provided that $\beta \approx 27°$ and $\alpha \approx 0.7°$. These conditions are optimal for the proper coupling of the transverse and longitudinal velocities in the gravitational field and provides for the reduction of the average atomic velocity to the lowest output value of 11 cm/s.

Fig. 9 shows the relative change of the averaged over the cross-section atomic phase-space density, ρ_{ph}/ρ_{ph0}, in the two-dimensional waveguide under consideration as a function of the coordinate z. The substantial rise of the phase-space density is due to narrowing of the spatial and velocity distributions of the atomic ensemble (the tapering of the waveguide and the cooling of the atoms) and also the accumulation of atoms in the narrow part of the waveguide.

2.4. 3D hornfiber

Consider now the behavior of an atomic ensemble in a hollow three-dimensional tapering curved waveguide

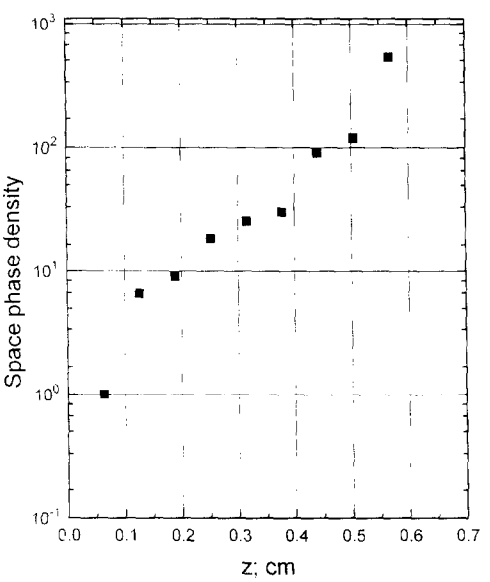

Fig. 9. Increase of the phase-space density of an atomic ensemble in a hollow 2D hornfiber. The increase is due to dissipative reflections of the atoms from the evanescent wave and the tapering waveguide geometry.

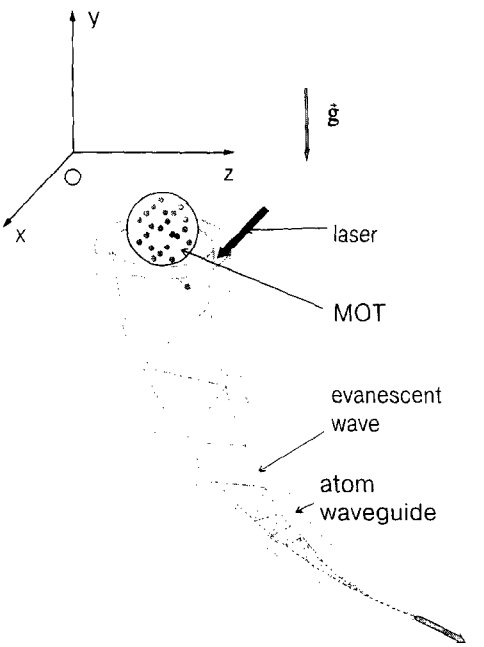

Fig. 10. Illustration of the use of a 3D hornfiber as a coherent source of de Broglie waves. Atoms are injected continuously from a magneto-optical trap into a hollow waveguide with an evanescent light wave formed on its inside surface with a positive frequency detuning with respect to the atomic absorption line. The atoms channel over the waveguide while undergoing reflections from the evanescent wave, some of which entail a reduction of the kinetic energy of the atoms. This causes the spatial and velocity distributions of the atomic ensemble to narrow, i.e., increases its coherence.

shown schematically in Fig. 10, along with a cloud of atoms confined in a magneto-optical trap (MOT). In this case we use the following parameters of evanescent light wave: $\Omega_R(r_{surface}) = 500$ MHz, $\delta = 100$ MHz. The cross-section of the 3D hornfiber by the XZ-plane is the 2D hornfiber defined previously. The channeling of atoms over such a waveguide may be due to their repeated reflections from an evanescent light wave. Assume that atoms are being continuously injected from a magneto-optical trap into the waveguide cavity and their velocity distribution corresponds to a Maxwell one with a temperature of $T = \hbar\Gamma/k_B$ (k_B being the Boltzmann constant) that can easily be attained in the trap. The entrance inside diameter of the waveguide corresponds to the characteristic size of the cloud of atoms in the trap and amounts to 500 μm. The diameter of the exit waveguide aperture is 10 μm. We computed the averaged over the cross-section phase-space density of the atomic trajectories in several planes parallel to the YOX plane. Fig. 11 presents the phase-space density normalized to its initial value $\rho_{ph}(z)/\rho_{ph0}$ as a function of the coordinate z. One can see

that while the atoms channel in the waveguide over a distance of $L \cong 1$ cm, their phase-space density is increased by five orders of magnitude. The larger increase (by more than two orders of magnitude) of the phase-space density in comparison with that in the case of a two-dimensional waveguide is explained by the additional narrowing of the spatial distribution and the longer lifetime of the atoms, which in the three-dimensional waveguide is about 1 second. Note that the total probability that a single atom will be lost in the 3D-hornfiber is of the order of 10^{-9}.

The average transverse atomic velocity in the ensemble at the exit of the waveguide amounts to about 10 cm/s, while the mean absolute velocity is around 20 cm/s. However, at the expected high densities of atoms in such a waveguide equalization of their kinetic energy distributions among all their degrees of freedom will take place because of collisions and long channeling time. Therefore, one might expect that the average atomic velocity will be around 10 cm/s, which corresponds to an ensemble temperature of $T = 1.5 \times 10^{-5}$ K. As will be demonstrated below, reaching such a low temperature at atomic densities of the order of 10^{14}–10^{15} cm^{-3} makes quantum statistics peculiarities to manifest themselves in the atomic system.

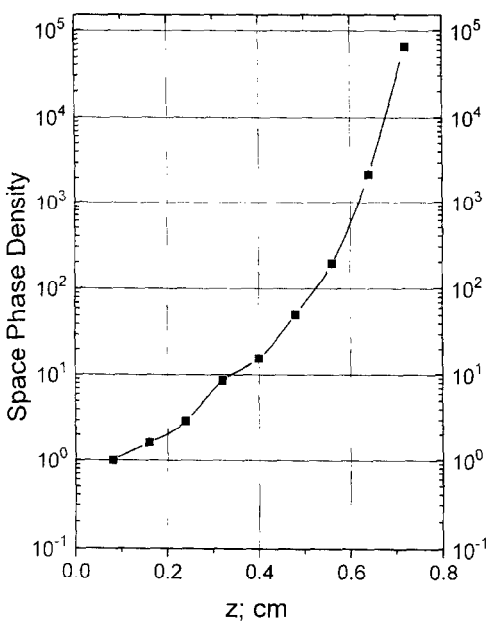

Fig. 11. Phase-space density of an atomic ensemble in a 3D hollow hornfiber as a function of the longitudinal coordinate. The narrowing of the spatial atomic distributions over the two coordinates by a factor of 50 approximately and the five-fold reduction of the width of the absolute atomic velocity distribution raises the phase-space density of the ensemble by five orders of magnitude. As in the two-dimensional case, this occurs thanks to the presence of dissipation in the system and the tapering geometry of the waveguide.

3. Results and discussion

The achievement of an extremely cold and dense ensemble of weekly interacting bosons gives an opportunity to use the proposed device for investigating quantum statistics phenomena and the wave propagation of matter. Consider a tapering waveguide terminating in a horizontal section of a cylindrical waveguide with an inside diameter of 4 μm. Assume that while channeling over it, an atom undergoes no spontaneous decays (there occur only elastic reflections of slow atoms from the evanescent wave with its frequency detuned far from resonance). Accordingly, there is no "repumping" laser light. Insofar as the temperature of the atomic ensemble is low, we assume that the probability of three-particle collisions is also low. Consequently, the Na_2 molecules can be disregarded.

3.1. Bose–Einstein condensate?

If the phase-space density of noninteracting bosons in an external potential exceeds a certain value governed by the form of the potential, a perceptible proportion of the particles in the ensemble will reside at the lowest energy level. This phenomenon, known as the Bose–Einstein condensation, gives rise to some interesting physical properties of the ensemble, associated with the high degree of coherence of the wave functions of individual atoms. A Bose–Einstein condensate is formed when the average distance between the particles in the ensemble becomes commensurable with the de Broglie wavelength.

Let us reveal the population pattern of the atomic waveguide modes. To this end, we use the results of Ref. [6] which presents an approximate equation for the radial-rotational energy levels of atoms propagating in a quantum fashion over a hollow cylindrical waveguide with an evanescent wave in the case where the atomic de Broglie wavelength is shorter than the optical wavelength, $\lambda_{dB} < \lambda$ (we assume that violating this condition affects very little the character of the mechanical action of light on the atom):

$$\sqrt{\frac{\epsilon_R}{E_{n,m}}}\,\frac{m^2}{U} - \frac{m\pi}{2} + \sqrt{\frac{E_{n,m}U^2}{\epsilon_R} - m^2} \times \left[1 - \frac{1}{U} + \frac{1}{U}\ln\left(2\sqrt{\frac{E_{n,m}}{V_{max}} - \frac{\epsilon_R m^2}{V_{max}}U^2}\right)\right] \approx \left(n + \tfrac{1}{2}\right)\pi. \tag{12}$$

Here n, $m = 0, 1, \ldots$, are the radial and rotational quantum numbers, respectively, V_{max} is the barrier height of the evanescent wave, U is a dimensionless parameter characterizing the penetration depth of the evanescent wave into the vacuum, and $\epsilon_R = 2\hbar^2U^2/Md^2$ is an energy of the same order of magnitude as the recoil energy. Eq. (12) was

numerically solved for $E_{n,m}$. In the system in hand, there is no longitudinal coordinate dependence, and so, for the sake of simplicity, let us examine a cylindrical waveguide section of fixed length $L = d$, assuming that the atomic wave functions go to zero at its ends ("blank" walls). Obviously the choice of the value of L is arbitrary and is only required to satisfy the condition $L \gg \lambda_{dB}$, for if the de Broglie wavelength λ_{dB} and the characteristic distance between the particles are much smaller than the size of the optical cavity, the physical properties of the ensemble of particles will be governed by its temperature and density and will depend weakly on the cavity geometry. The total kinetic energy of an atom in the waveguide is the sum of the total energies of the radial-rotational and translational atomic motions:

$$E_{n,m,l} = E_{n,m} + E_l = E_{n,m} + \frac{\pi^2 \hbar^2 l^2}{8ML^2}, \tag{13}$$

where $l = 1, 2, \ldots$, is the translational quantum number characterizing the motion of the atom along the waveguide [19]. Let 10% of the total number of atoms confined in the magneto-optical trap, $N_{MOT} \cong 10^{10}$ atoms [21], enter the waveguide cavity every second, this corresponds to an atomic flow of $j_{in} = 10^9$ atoms/s. Inasmuch as the flow j remains approximately constant (the loss of atoms is low), the density of the atomic ensemble in the cylindrical part of the waveguide is $\rho = j/vS = 4j\tau/\pi Ld^2 \cong 10^{14}$ cm^{-3}, where v is the velocity of the collective motion of the atoms along the waveguide. The distribution of the atoms among the waveguide energy levels $E_{n,m,l}$ is defined by the Bose function

$$f_{Bose}(E) = \left[\exp\left(\frac{E_{n,m,l} + \mu}{k_B T}\right) - 1\right]^{-1}, \tag{14}$$

where μ is the chemical potential of the system depending on the number of particles, $N = \rho(\pi d^2/4)L$, and the temperature T, which we found numerically from the normalization equation

$$\sum_{n,m,l} f_{Bose}(E_{n,m,l}) = N. \tag{15}$$

Fig. 12 presents the relative population $G = N_0/N$ of the minimum-energy mode of the waveguide as a function of the number of particles in the magneto-optical trap, N_{MOT}, where N_0 is the number of atoms in the fundamental waveguide mode. One can see that at a certain number density of the particles, reached with realistic N_{MOT} values, there occurs a sharp increase in the proportion of atoms in the fundamental waveguide mode. The system parameters being what they are, the relative population of the fundamental mode amounts to a few percent, which may impart the ensemble some new properties typical of a Bose–Einstein condensate. Note, however, the existence of numerous factors capable of preventing the attainment of sufficiently high particle densities and the formation of a

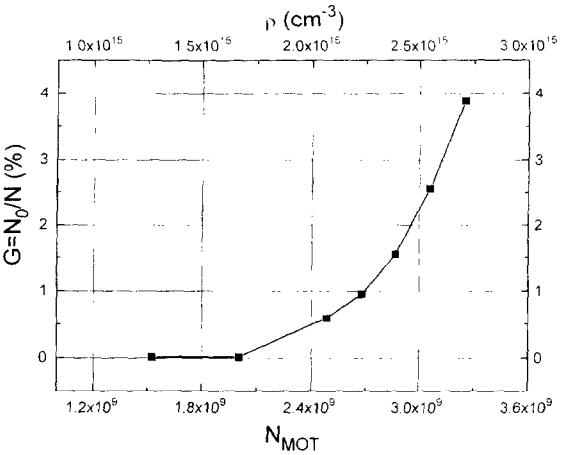

Fig. 12. Relative population of the fundamental mode of a cylindrical waveguide with a diameter of $d = 4$ μm, in which a 3D hornfiber terminates, as a function of the number of atoms confined in a magneto-optical trap, of which 10% are being injected every second into the hornfiber. The concentration of atoms in the waveguide is plotted on the top X-axis. Attaining a fundamental-mode population at a level of a few percent will enable one to study quantum statistics specifics for bosons, and use the scheme suggested as a bright coherent source of de Broglie waves.

Bose–Einstein condensate. These include the already noted three-particle collisions giving rise to the Na_2 molecules, interatomic collisions in the evanescent light wave leading to the $|F = 1\rangle \leftrightarrow |F = 2\rangle$ transitions, and excitation by diffuse light.

3.2. Bright coherent source of de Broglie waves

The proposed device can be used as a very bright source of ultracold atoms. The output atomic flux is equal to the input one because of loss of atoms propagating through the fiber can be made as small as desired. The average velocity $\langle v \rangle$ of the atomic output beam is 10 cm/s, the corresponding de Broglie wavelength of the atoms is $\lambda_{dB} \cong 0.2$ μm. The divergence of the atomic beam issuing from the waveguide is determined by its transverse temperature and is about $\pi/2$ rad. In the case the initial flux is 10^9 atoms/s, the brightness of the output beam $B = j_{out}/2\alpha \cong 3 \times 10^8$ atoms/s · sr.

Since a perceptible proportion of atoms in the output section of the waveguide are in one and the same quantum state, such a waveguide can be viewed as a coherent source of de Broglie waves. Let us estimate the main parameters of the source suggested. The coherent output flow of atoms in the lowest energy mode is $j_{out}^{coh} = j_{in}G = 4 \times 10^7$ atoms/s and its divergence is determined by diffraction. Creating a coherent source of such high brightness will make possible many interference experiments on atomic optics.

Note also that by using the method suggested, one can drive a classical atomic ensemble at a temperature and particle density typical of a magneto-optical trap to a quantum state with a high degree of coherence. This will make it possible to study the specific features of the quantum mode of propagation of atoms over the waveguide, particularly the character of the mechanical action of light on atoms whose de Broglie wavelength is commensurable with the optical wavelength. Reaching high particle densities in the system will enable one to reveal the molecule formation dynamics at very low temperatures.

One of the important problems that the experimentist is faced with in implementing the source suggested is the extraction of the atomic beam from the waveguide. While overlapping and interacting with the atomic beam, the laser beam producing the evanescent wave may substantially impair the coherence of the atomic ensemble. One way to solve this problem is to make the waveguide terminate in a greatly diverging funnel, so that the light beam emerges within a hide-angle cone, and use a diaphragm to separate the light of the atomic beam from each other. Another possible method is to suppress the evanescent wave in the exit section of the waveguide cooled to a temperature close to that of liquid helium by applying an antireflection or absorbing coating onto the outer surface of the waveguide. In that case, ultracold atoms will traverse this short waveguide section without suffering any dramatic heating and retaining their coherence, for the energy exchange between the phonon quantum system of the dielectric and the atom with de Broglie wavelength much in excess of the characteristic atom dielectric interaction length is of very low probability.

Acknowledgements

The authors are grateful to Yu.E. Lozovik for useful discussions of the results. This work was supported by the Russian Basic Research Foundation (Project No. 95-02-05350), the Russian State Scientific-Technological Program 'Fundamentalnaya Metrologiya' (Fundamental Metrology) (Project No. 272 Atom), and the US Ministry of Energetics through the intermediary of the University of Arizona.

References

[1] C.S. Adams, M. Sigel, J. Mlynek, Phys. Rep. 240 (1994) 143.
[2] V.I. Balykin, V.S. Letokhov, Atom Optics with Laser Light, in: Laser Science and Technology, An International Handbook (Harwood, 1995).
[3] J.P. Dowling, J. Gea-Banacloche, Quantum atomic dots, Adv. At. Mol. Opt. Phys., to be published.
[4] M.A. Ol'shanii, Yu.B. Ovchinnikov, V.S. Letokhov, Optics Comm. 98 (1993) 77.
[5] M.J. Renn, D. Montgomery, O. Vdolin, Z.D. Anderson, C.E. Wieman, E.A. Cornell, Phys. Rev. Lett. 75 (1995) 3253.
[6] S. Marksteiner, C.M. Savage, P. Zoller, S. Rolston, Phys. Rev. A 50 (1994) 2680.
[7] M.J. Renn, E.A. Donley, E.A. Cornell, C.A. Wieman, D.Z. Anderson, Phys. Rev. A 53 (1996) 1.
[8] R.J. Cook, R.K. Hill, Optics Comm. 43 (1982) 258.
[9] S.M. Tan, D.F. Walls, Phys. Rev. A 50 (1994) 1561.
[10] V.I. Balykin, V.S. Letokhov, Yu.B. Ovchinnikov, A.I. Sidorov, Pis'ma ZETF 45 (1987) 282.
[11] M. Kazevich, P.S. Weiss, S. Chu, Optics Lett. 15 (1990) 607.
[12] C.G. Aminoff, A.M. Steane, P. Bouyer, P. Desbiolles, J. Dalibard, C. Cohen-Tannoudji, Phys. Rev. Lett. 71 (1993) 3083.
[13] Yu. Ovchinnikov, D.V. Laryushin, V.I. Balykin, V.S. Letokhov, Pis'ma ZETF 62 (1995) 102.
[14] Yu. Ovchinnikov, J. Soding, R. Grimm, Pis'ma ZETF 61 (1995) 23 [JETP Lett. 61 (1995) 10].
[15] J. Soding, R. Grimm, Yu.B. Ovchinnikov, Optics Comm. 119 (1995) 652.
[16] E.A. Cornal et al. (private communication).
[17] V.I. Balykin, D.V. Laryushin, M.V. Subbotin, V.S. Letokhov, Pis'ma ZETF 63 (1996) 763.
[18] J. Dalibard, C. Cohen-Tannoudji, J. Opt. Soc. Am. B 6 (1989) 2023.
[19] V.I. Balykin, V.S. Letokhov, Appl. Phys. B 48 (1989) 517.
[20] D.V. Laryushin, Yu.B. Ovchinnikov, V.I. Balykin, V.S. Letokhov, Optics Comm. 135 (1996) 138.
[21] K.B. Davis, M. Mewes, M.A. Joffe, M.R. Andrews, W. Ketterle, Phys. Rev. Lett. 74 (1995) 5202.